separations

MDPI

Review

Research Progress on Adsorption and Separation of Petroleum Hydrocarbon Molecules by Porous Materials

Haibin Yu [1], Jiazhong Zang [1], Chunlei Guo [1], Bin Li [1,*], Ben Li [1], Xueyin Zhang [2] and Tiehong Chen [2]

[1] CenerTech Tianjin Chemical Research & Design Institute Company, Ltd., Tianjin 300131, China
[2] School of Materials Science and Engineering, Nankai University, Tianjin 300350, China
* Correspondence: libin52@cnooc.com.cn

Abstract: Petroleum is an indispensable chemical product in industrial production and daily life. The hydrocarbon molecules in petroleum are important raw materials in the organic chemical industry. The hydrocarbons currently used in industry are usually obtained by fractional distillation of petroleum, which not only consumes more energy, but has poor separation selectivity for some hydrocarbons. Adsorption separation technology has many advantages such as energy saving and high efficiency. It can adsorb and separate hydrocarbon molecules in petroleum with low energy consumption and high selectivity under mild conditions. In this paper, the research progress of adsorption and separation of hydrocarbon molecules in petroleum is reviewed, and various new catalysts and the rules of adsorption and desorption are analyzed.

Keywords: petroleum; hydrocarbon molecules; adsorption and separation; porous materials

check for updates

Citation: Yu, H.; Zang, J.; Guo, C.; Li, B.; Li, B.; Zhang, X.; Chen, T. Research Progress on Adsorption and Separation of Petroleum Hydrocarbon Molecules by Porous Materials. *Separations* **2023**, *10*, 17. https://doi.org/10.3390/separations10010017

Academic Editor: Sascha Nowak

Received: 20 September 2022
Revised: 09 October 2022
Accepted: 17 October 2022
Published: 29 December 2022

Copyright: © 2022 by the authors. Licensee MDPI, Basel, Switzerland. This article is an open access article distributed under the terms and conditions of the Creative Commons Attribution (CC BY) license (https://creativecommons.org/licenses/by/4.0/).

1. Introduction

In recent years, with the increasingly serious global greenhouse effect and climate and environmental problems, the construction of an environmental governance system and redistribution of the energy structure have raised the focus of attention [1–3]. Further development has become a new challenge. The petrochemical industry and related manufacturing industries are an extremely important part of the huge industrial system and have an important impact on social development. A series of environmental problems brought about by the petroleum industry also need to be solved urgently. How to effectively adjust the relevant industrial structure, further realize the high-value and clean energy industry line and implement the sustainable development route are major problems faced by major enterprises in the industry [4].

Petroleum is a viscous, dark brown liquid with a flowing or semi-flowing state. It belongs to the same fossil fuel as coal and has a wide range of industrial applications [5,6]. Petroleum is mainly composed of two elements, carbon and hydrogen, and simultaneously contains trace amounts of other elements such as sulfur, oxygen, and nitrogen. The major constituents in petroleum or its straight-run products are hydrocarbons such as alkanes, naphthenes, and aromatics. Hydrocarbons are also present in secondary processed products of petroleum or other petroleum products. These hydrocarbon molecules are important raw materials in the organic chemical industry. Monocyclic aromatic hydrocarbons are important raw materials for the production of synthetic rubber, synthetic fibers, and synthetic resins [7]. The cost of direct synthesis of hydrocarbon molecules is too high, therefore, the hydrocarbons used in industry are usually obtained by separating coal or petroleum.

Since there are more than 300 kinds of hydrocarbons in petroleum, the separation of various components to satisfy different industrial needs is an important issue in chemical production [8]. Fractionation technology is one of the commonly used methods to separate hydrocarbons from petroleum. Different types of hydrocarbon molecules have different molecular chain lengths, which leads to their different boiling points. Fractionation techniques

utilize differences in the boiling points of different hydrocarbons to achieve separation. The shorter the molecular chain of organic matter, the lower the boiling point, the longer the molecular chain, the higher the bpetroleuming point. The main device used in fractionation technology is a fractionation tower. In the fractionation tower, the temperature varies from area to region, which makes hydrocarbon molecules with different boiling points condense into liquid fractions at different heights. During the fractionation operation, the petroleum vapor is passed into the fractionation tower at a high temperature, and height affects the type of product deposition, so as to achieve the purpose of separating hydrocarbon molecules [9]. For the azeotropic mixture, a series of special rectification methods such as extractive rectification, azeotropic rectification, and pressure swing rectification can also be used for separation. These processes are all physical change processes, and the separated hydrocarbon molecules can be used in different chemical production activities. In addition, long-chain hydrocarbons can be further processed by thermal cracking or hydrocracking to produce short-chain hydrocarbons, however, the fractional distillation technology also has certain limitations [10]. For example, some hydrocarbon molecules, such as n-paraffin, have a long boiling range, and there are many isomers with boiling points close to n-paraffin in the raw material. It is impossible to use the rectification method to realize the separation of n-paraffins. These limitations indicate that a new separation method is urgently needed in the field of petroleum separation.

At the same time, the pollutants caused by petroleum spills are also difficult to be separated by conventional methods [11–13]. They are usually highly lipophilic, semi-volatile, and accumulated in water, which bring great pollution to local water sources due to their non-biodegradability and persistence, especially polycyclic aromatic hydrocarbons and phenols. when present in living cells, they can bioaccumulate and biomagnify through the food chain and enter the human body [14], therefore the separation of these aromatics from contaminants is particularly important.

Adsorption separation technology has many advantages such as energy saving and high efficiency, which has attracted extensive attention in the research field. The principle of adsorption separation is that when the liquid petroleum is in contact with a porous material with a large surface area, hydrocarbon molecules smaller than the diameter of the pore of the adsorbent will enter the pore. After the adsorption is completed, the adsorbed molecules can be desorbed by changing the conditions to obtain the target product. For example, in the separation of aromatic hydrocarbons, high-purity aromatic hydrocarbons can be obtained by using a desorbent to desorb the adsorbed aromatic hydrocarbon components after the adsorbent selectively adsorbs the aromatic hydrocarbons. The obtained high-purity aromatics can be used as high-aromatic solvent oil or heavy aromatics resources, while the remaining products such as high-purity non-aromatic components can be used as clean diesel with excellent combustion performance [15]. In addition, 5A molecular sieves are commonly used in industry for the adsorption and separation of n-alkanes, and for which the effective pore size of this molecular sieve is 0.51 nm. On the contrary, cycloalkanes and aromatics will not enter the pores [16]. Apart from this, there are many other adsorbents used for the separation of different components, such as mesoporous silica, metal-organic frameworks (MOFs), and polymeric adsorbents. More importantly, adsorption separation has been applied in industrial production. For example, the simulated moving bed adsorption separation technology is an effective method for n-paraffin separation [17]. This method has many significant advantages, such as high separation efficiency and low energy.

2. Introduction to Adsorption Separation Technology

Adsorption refers to the phenomenon that specific components in the mixture are enriched on the surface of the adsorbent under the action of the adsorbent. Adsorption can be divided into physical adsorption and chemical adsorption. Physical adsorption is a reversible process, which mainly depends on the van der Waals force between molecules. However, chemisorption is mostly irreversible, which depends on the formation or breaking of chemical bonds between atoms. In industry, adsorption and separation technology uses specific solid adsorption materials to selectively adsorb gaseous or liquid mixed

components to separate the components that can be adsorbed by adsorbents and those that cannot be adsorbed by adsorbents.

There are many kinds of adsorption materials used in the adsorption reaction. From the reaction mechanism, they can be divided into shape selective adsorption materials, complex adsorption materials, and polar selective adsorption materials.

2.1. Shape Selective Adsorption Materials

The most important representative of shape-selective adsorption materials is a molecular sieve and porous materials. The so-called shape-selective catalysis refers to the selective adsorption performance of molecular sieves, that is, molecular sieving is carried out according to the size and shape of molecules in the adsorption process. Different types of porous materials have different pore sizes, which can be matched with molecules of different sizes. Only the molecules matching the pore size of porous materials can be adsorbed and separated. We can select porous materials with an appropriate pore size as adsorbents to meet the needs of different types of reactions according to the kinetic diameter of the molecules to be adsorbed.

The pore steric hindrance effect of molecular sieves can be well used for shape-selective screening of alkanes, cycloalkanes, or aromatics in oil products. For example, the commonly used FAU, BEA, and LTL molecular sieves are widely used in petrochemical catalysis because of their suitable solid acidity and texture structure [18]. Ban et al. [19] used different types of molecular sieves, such as mordenite, β, and Y zeolite to perform the adsorption and separation of benzene in a benzene/propylene mixture. The research results of adsorption selectivity showed that β, MCM22, and MOR zeolites have high selectivity for benzene, and the adsorption performance has good stability. While Y zeolites show low benzene adsorption at low temperature and low pressure, indicating that the molecular sieves with different texture types have different selectivity for hydrocarbon molecules.

2.2. Complex Adsorption Materials

Complex adsorption materials mainly use π complex bond between adsorbent and adsorbate for adsorption [20]. π complex bond has better selectivity, which belongs to the category of a weak chemical bond, but its force is usually much larger than van der Waals force and electrostatic force, The complex adsorption materials can be roughly divided into Cu type and Ag type complexing agents, whose synthesis process usually adds Cu (II) or Ag ions to molecular sieves or activated carbon supports by impregnation or ion exchange. Gao [21] synthesized CuCl/Y molecular sieve by monolayer dispersion method with $CuCl_2$ as a precursor. When the copper loading is 5 mmol g^{-1}, with the presence of CO_2, CH_4, N_2, and other interfering gases, the adsorption capacity of CO can reach 3.03 mmol g^{-1} and its selectivity factor can still reach 2.83, 24.73, and 68.00, respectively. This kind of adsorbent has a good performance in separating gaseous mixtures.

The principle of π complex adsorption [22] is to achieve adsorption by using the coincidence of the adsorbate orbit and the transition metal ion orbit on the adsorbent to form a π complex bond. Theoretically, all d-group transition metals can form π complex bonds. However, since few elements can both give and release electrons simultaneously, there are only Cu^+ and Ag^+ in practical application, which have also become the main research objects of this kind of material.

2.3. Polarity Selective Adsorbent

Polar selective adsorption materials are widely used in practical production because of their simple and convenient synthesis method, recyclability, and high economic value. The main representatives of these materials are activated carbon, alumina, molecular sieve, etc., which are characterized by ultra-high pore size, specific surface area, and surface degree points [23]. Thus, they are widely used in waste gas treatment, wastewater treatment, and other fields. Taking the common activated carbon as an example, it has a large number of pore structures, including V-shaped pores, and uniformly fractured pores [24], and the rich pores provide a large number of reactive active sites for the activated carbon. At the same

time, the performance of activated carbon can be further improved by loading functional groups on its surface. Qu [25] studied the adsorption principle and process of nitrogen and sulfur heterocycles in liquid hydrocarbons by introducing organic groups on the carbon surface.

In the absence of oxygen-containing functional groups on the surface, the adsorption of such materials mainly depends on π-π stacking interaction, and the affinity for adsorbates depends on the size of the π system. Therefore, the selectivity and capacity for hydrocarbon molecules will be greatly improved. For materials with a large number of oxygen-containing functional groups on the surface, the adsorption depends on the acidic sites on the surface and π-H interaction, and its adsorption performance will change with the introduction of different functional groups. Pang et al. [26]. reported that a water-soluble conjugated polyelectrolyte ($PBCSO_3Na$) was used to prepare the $PBCSO_3Na$/graphene composite sensor. The conjugated polyelectrolyte can also be used as an organic intermediate layer to improve electron transfer. Because the polar groups attached to the main chain can form dipoles at the electrode interface, thus minimizing the interface energy barrier [27], which is conducive to the adsorption of aromatic hydrocarbons by multilayer graphene to monitor the content of aromatic hydrocarbons with high sensitivity.

The adsorption principle of molecular sieves is to use the acidic sites on the surface. The tri-coordinated Al in the framework is used as the Lewis acid acceptable electron pair, while the aromatic hydrocarbon in the hydrocarbon molecule is the π electron donor. As a Lewis base, it can interact with the Lewis acid active sites in the adsorbent to form coordination bonds, which can be attached to the adsorbent surface through chemical adsorption. Costa et al. [20] used molecular sieves rich in Lewis acid active sites to carry out adsorption tests on different kinds of polycyclic aromatic hydrocarbons and proved that Lewis acid active sites have a good adsorption effect on π electrons.

3. Research Progress on Adsorption and Separation of Hydrocarbon Molecules

The most important composition of petroleum is hydrocarbon molecules, and each composition is shown in Table 1. Therefore, the essence of studying the adsorption and separation of petroleum components is to study the adsorption and separation of hydrocarbon molecules by adsorbents. At the same time, petroleum hydrocarbon pollutants are difficult to degrade compounds, and are listed as priority pollutants [28]. Human petroleum industry activities and accidental leakage will cause petroleum hydrocarbon pollution, and pose direct or indirect health risks to all life forms on Earth [29,30]. Therefore, the adsorption and separation of petroleum components have become an important issue. The following is a classification and summary of the recent adsorption and desorption laws of hydrocarbon molecules.

3.1. n-Alkanes

Straight or branched chain (acyclic structure) n-paraffins or isoparaffins are the main components in petroleum fractions. Octane number is an important measure of the anti-knock ability during gasoline ignition. Under normal circumstances, due to the low octane numbers of n-paraffins and high octane numbers of isoparaffins, aromatic hydrocarbons, and naphthenes, the separation of n-paraffins is beneficial to improve the octane number of gasoline [31]. According to the above-mentioned, a molecular sieve is the adsorbent to achieve selective adsorption depending on the molecular size of different components in the mixture and the affinity with the acid site and the internal diffusion effect [32–34]. It can adsorb alkane cations such as $C_3H_7^-$, and basic sites are used to adsorb H^+. Among many kinds of molecular sieves, the effective pore size of molecular sieve 5A between the kinetic diameters of n-alkanes and isoparaffins is widely used in the separation of n-alkanes.

Table 1. Contents of components in naphtha [35].

Component	n-Alkanes	Isoparaffin	Olefins	Cycloparaffin Aromatics		Total
content%	27.92	30.42	0.02	28.85	12.78	100

Cao [35] used molecular sieve 5A as an adsorbent for the adsorption and desorption of n-alkanes in naphtha. A series of experiments were carried out under different conditions to explore the influence of various factors on the adsorption and desorption performance. Adsorption experiments were carried out at different temperatures to explore the effect of temperature on the adsorption and desorption performance. Figure 1 shows the content of n-alkanes in the raffinate after the adsorption is completed. It can be seen that when the temperature is lower than 180 °C, the content of n-alkanes in the raffinate of the reaction system gradually decreases with increasing of the adsorption temperature, and this indicates that in this temperature range, the adsorption performance will increase with the increase of adsorption temperature. Through the desorption tests at different temperatures, Figure 2 shows the content of n-paraffins in the desorption liquid during the desorption process carried out at different temperatures. It can be seen that in the whole temperature range, the desorption efficiency is positively correlated with the temperature, which is basically consistent with the adsorption rule.

Figure 3 shows the effect of different space velocities on the adsorption and desorption performance, it can be seen that the molecular sieve has an obvious difference in the adsorption effect of the adsorbate at different space velocities and molecular sieve 5A exhibits obvious desorption effect of alkane at a 12 h^{-1} space velocity. In order to explain the effect of space velocity on the adsorption capacity more conveniently, the researchers also studied the relationship between the oil/molecular sieve ratio and the content of n-paraffins (carbon chain length 6–9) in the system after the adsorption is completed under different space velocities. The results obtained are shown in Figure 4. This means that to achieve the same separation effect, the minimum amount of molecular sieve is required when the space velocity is 0.0025 h^{-1}, which indicates that the optimal space velocity for adsorption is 0.0025 h^{-1}. During the whole cycle of adsorption-desorption of n-alkanes, the optimum temperature for molecular sieve 5A was 180 °C, the optimum space velocity for adsorption was 0.0025 h^{-1}, and the optimum space velocity for desorption was 12 h^{-1}.

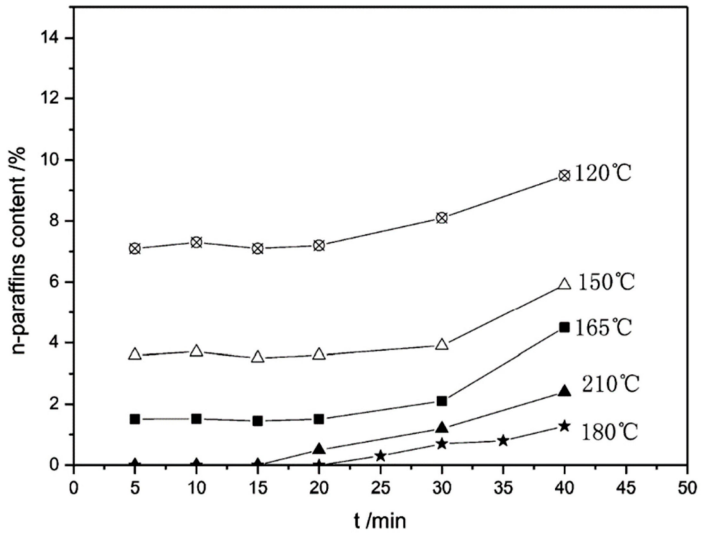


Figure 1. The content (%) of n-alkanes in the raffinate at different temperatures [35].

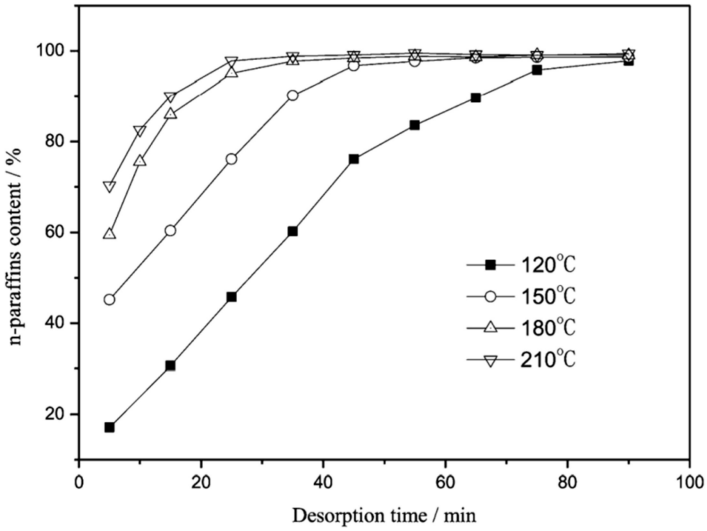


Figure 2. The content (%) of n-alkanes in the desorbed liquid at different temperatures [35].

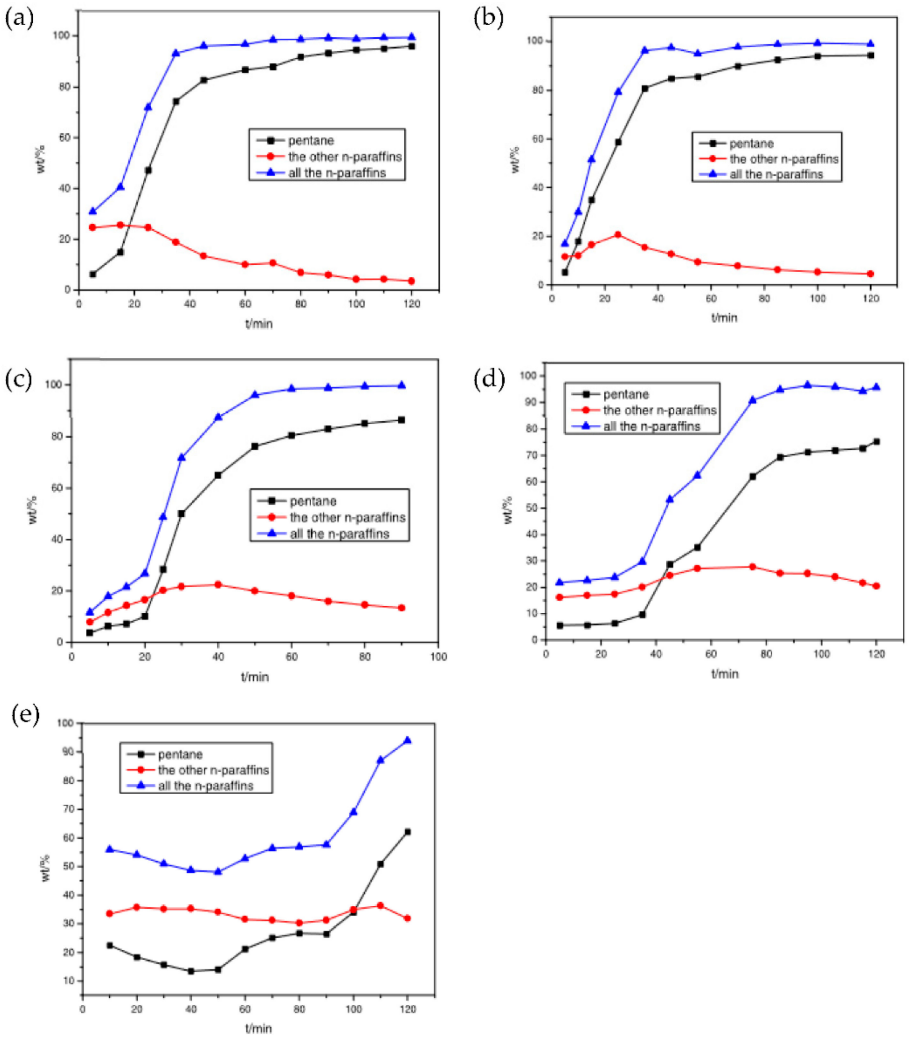


Figure 3. Relationship between desorption time and n-paraffin content at different space velocities [35]. (**a**) 25 h^{-1} (**b**) 18 h^{-1} (**c**) 12 h^{-1} (**d**) 7 h^{-1} (**e**) 3.5 h^{-1}. Space velocities: The amount of hydrocarbons passing through 5A catalyst per unit time.

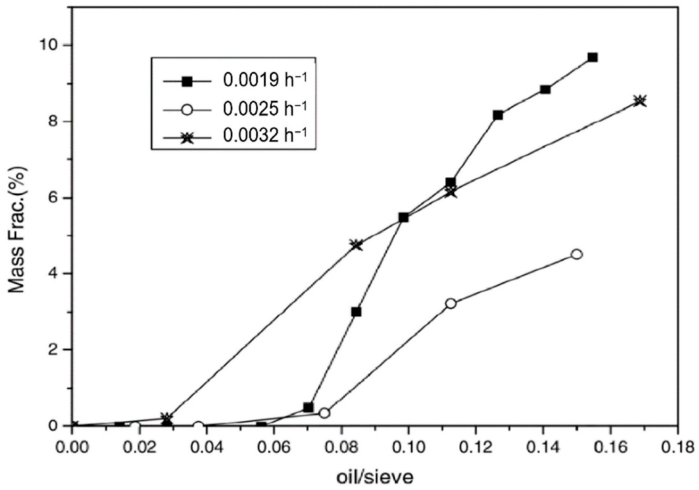


Figure 4. Relationship between oil/sieve ratio and n-paraffin mass fraction at different space velocities [35]. Oil/sieve ratio: raffinate oil/molecular sieve.

In addition, Liu [36] used pulse experiments to study the adsorption and separation of n-alkanes between 10 and 16 carbon atoms by molecular sieve 5A. They used gas chromatography to analyze the sample, taking the injection volume of the desorption solution as the abscissa and the mass fraction of various hydrocarbon components as the ordinate (The mass fraction of each alkane in pulse solution and desorption solution is 5%, and isooctane is used as diluent for the rest). The degree of separation R is calculated to represent the separation effect of n-alkane and 2-methylentane.

The pulse curves and corresponding data of $nC_{11–16}$ at different adsorption temperatures are shown in Figure 5 and Table 2, respectively. At 120 °C, with the increase of carbon chain length, the value of ΔV_R decreased significantly, and the peak gradually widened, that is, the value of $W_{1/2}$ gradually increased, which indicated that the adsorption performance of n-alkanes with a long carbon chain was poor, and the adsorption rate was slow at this temperature. When the temperature gradually increased to 180 °C, ΔV_R gradually increased and reached the maximum value, and the value of $W_{1/2}$ also gradually decreased, indicating that the adsorption capacity and adsorption rate for $nC_{11–16}$ were significantly improved. However, when the temperature reached 200 °C, the value of ΔV_R decreased, and the value of R also reached the maximum, indicating that the adsorption capacity began to weaken. Therefore, it could be concluded that the optimal adsorption temperature for the separation of n-alkanes by 5A molecular sieve was 180 °C, which was also the same as the previous report by Gao's group.

For desorption, the choice of desorbent is also important, which has a great influence on adsorption and desorption performance. The ΔV_R, $W_{1/2}$, and R values of $nC_{10–16}$ when n-alkanes with different chain lengths were used as desorbents are shown in Figure 6. According to Figure 6a, it could be seen that when the carbon number is 5–8, the ΔV_R value of $nC_{10–13}$ first increased and then decreased, and it reached the maximum value when the number of carbon atoms was 7, while for $nC_{14–16}$, the value obviously showed a decreasing trend. In Figure 6b, the value of $W_{1/2}$ of $nC_{10–13}$ floats a little bit, indicating that its adsorption rate was less affected by the carbon chain length of the desorbent, while the value of $nC_{14–16}$ was gradually decreased, indicating that the increase of the carbon number of desorbent is conducive to desorption. Finally, according to Figure 6c, it could be seen that although the R values of n-alkanes with different carbon numbers change differently, they all reach the maximum value when the carbon number is 7. To sum up, when nC_7 is used as desorbent, $nC_{10–16}$ has better desorption performance.

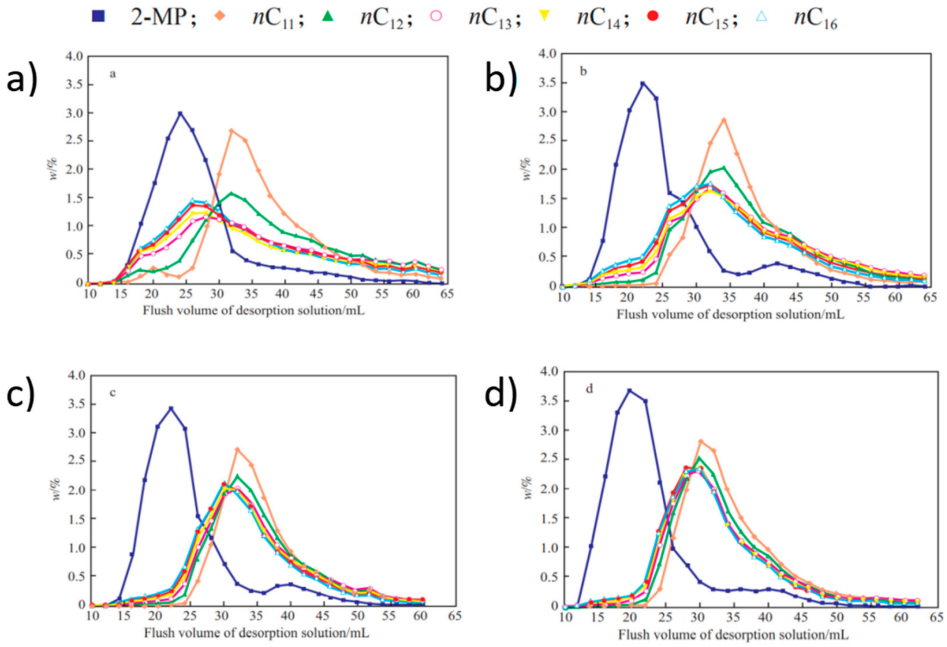


Figure 5. Pulse spectra of $nC_{11–16}$ at different adsorption temperatures [36]. (**a**) 120 °C (**b**) 150 °C (**c**) 180 °C (**d**) 200 °C.

Table 2. Pulse data of $nC_{11–16}$ at different adsorption temperatures [36].

Item	Temperature/°C	nC_{11}	nC_{12}	nC_{13}	nC_{14}	nC_{15}	nC_{16}
ΔV_R/mL	120	9.56	10.28	7.84	4.83	4.45	3.88
	150	12.20	12.33	12.84	12.48	10.89	9.91
	180	11.74	11.19	10.65	10.25	9.77	9.62
	200	11.75	10.77	10.12	9.79	9.61	9.78
$W_{1/2}$/mL	120	10.64	17.10	22.38	19.47	18.45	17.44
	150	9.67	14.41	18.50	18.98	16.67	15.65
	180	9.25	11.01	12.43	12.44	11.99	11.91
	200	10.22	10.91	11.48	11.67	11.61	11.73
R	120	0.90	0.74	0.48	0.32	0.31	0.28
	150	1.29	1.04	0.93	0.88	0.84	0.80
	180	1.31	1.14	1.01	0.98	0.95	0.94
	200	1.21	1.07	0.98	0.94	0.92	0.94

ΔV_R: net retention volume; $W_{1/2}$: half width; R: degree of separation. $W_{1/2}$: half peak width of envelope line in each group; a parameter characterizing the mass transfer rate; V_R: the retention volume of the component in the adsorption column; ΔV_R: the difference between V_R and 0 point of an n-alkane component or the net retention volume of the component; The results show the adsorptive capacity of 5A molecular sieve for this component; R: degree of separation.

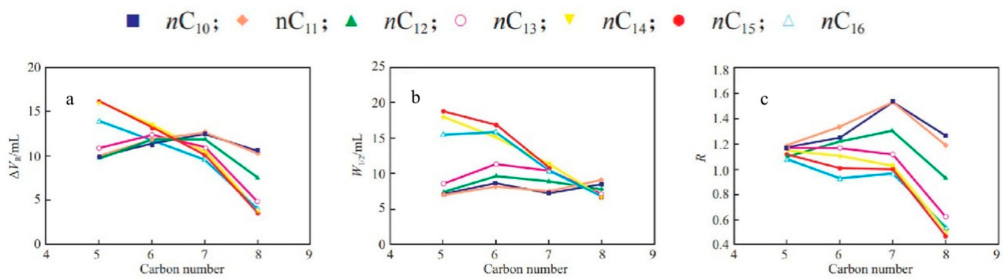


Figure 6. Pulse parameters of $nC_{10–16}$ when n-alkanes with different carbon numbers are used as desorbents [36] the values of (**a**) ΔV_R (**b**) $W_{1/2}$ (**c**) R.

The relationship between the ΔV_R, $W_{1/2}$, R values of $nC_{10–16,}$ and the water content of the adsorbent was shown in Figure 7. It could be seen from Figure 7a that the ΔV_R of $nC_{10–16}$ decreased gradually with the increase of the water content of the adsorbent, indicating that the water content of the adsorbent may be unfavorable for the adsorption of n-alkanes. This was mainly due to the fact that water molecules occupied the micropores of molecular sieves, reducing the adsorption volume and active sites of the adsorbent. From Figure 7b, it was found that the $W_{1/2}$ of $nC_{10–16}$ decreased firstly and then increased, and reached the minimum value when the adsorbent moisture content was 3.3%, especially for n-alkanes with carbon number larger than 12, indicating that the water content of adsorbent could improve the rate of adsorption and desorption to a certain extent. This may be due to the improved mass transfer of $nC_{10–16}$ in a 5A molecular sieve driven by water polarization [37]. As shown in Figure 7c, the R-value decreased with the increase of water content when the carbon number was 10–11, but only slightly decreased before 3.3%. When the carbon number is between 12 and 16, the R-value first increased and then decreased, reaching a maximum value of 3.3%. In conclusion, $nC_{10–16}$ exhibited the most excellent adsorption and separation performance with a water content of 3.3%.

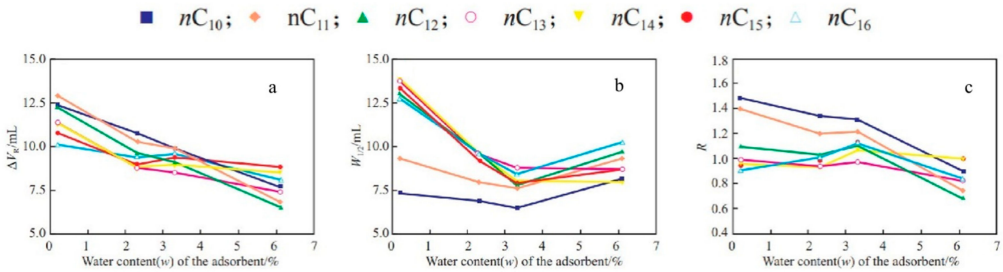


Figure 7. Relationship between pulse parameters of $nC_{10–16}$ and water content of adsorbent [36] the values of (**a**) ΔV_R (**b**) $W_{1/2}$ (**c**) R.

It has been confirmed that the Ca^{2+} exchange degree of the adsorbent has an effect on the adsorption and desorption performance. Figure 8 showed the effect of the replacement percentage of Na^+ by Ca^{2+} in the molecular sieve on the adsorption performance. As the ionic radius of Ca^{2+} is larger than that of Na^+, the six-membered ring of the A-type molecular sieve will be partially replaced by an eight-membered ring when a substitution occurs [38]. When the exchange degree of Ca^{2+} of the adsorbent was between 70.8% and 85.5%, the pulse spectrum showed no obvious difference. However, when the exchange is too high and exceeds 91.9%, the adsorption and desorption curve of $nC_{13–16}$ gradually slowed down, which is consistent with the view in the above reference that the hindering force of the long-chain alkanes is too large when the Ca^{2+} exchange of the adsorbent is too high.

Flush volume of desorption solution: The saturated adsorbent needs to be flushed with pulsed liquid to record the sample fraction, and the experiment was performed by recording every 2 mL.

In summary, starting from short-chain n-alkanes ($C_{5–7}$) and long-chain n-alkanes ($C_{10–16}$), the researchers studied the effects of temperature, space velocity, desorbent, water content, and Ca^{2+} exchange degree on the adsorption and desorption performance of n-alkanes. The adsorption and desorption regular of 5A type molecular sieves on n-alkanes under different conditions were comprehensively discussed, which provides a basis for further research on the adsorption and desorption laws of n-alkanes.

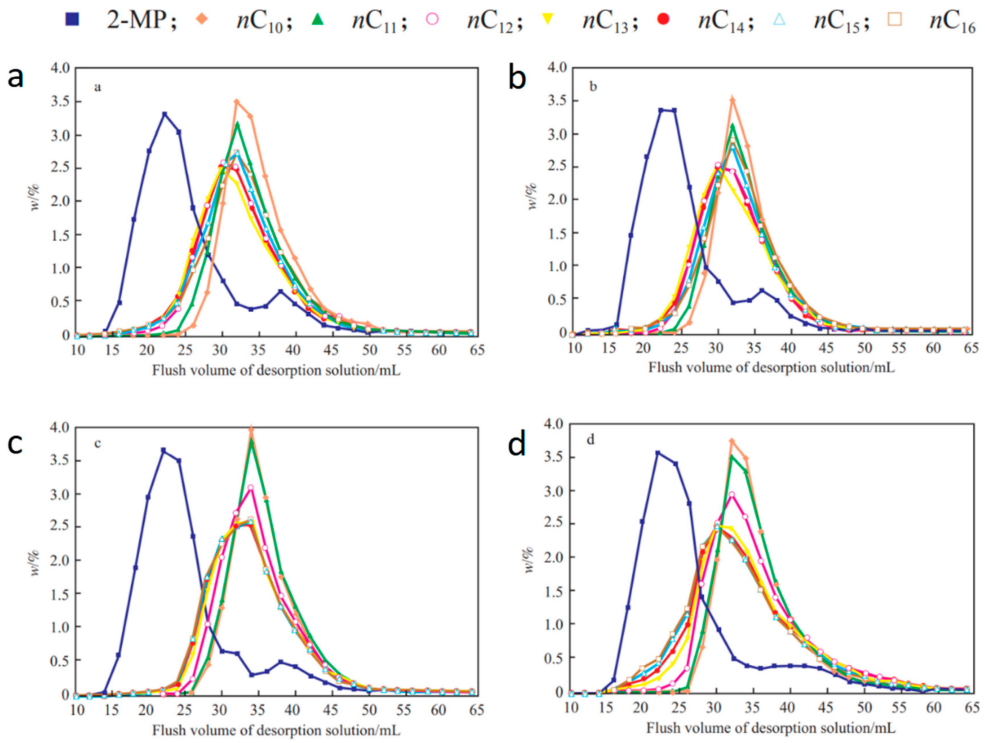


Figure 8. Pulse spectra of adsorbent Ca^{2+} exchange degree [36] (**a**) 70.8% (**b**) 85.5% (**c**) 91.9% (**d**) 97.5%.

In addition to the influence of external conditions on the adsorption performance, the structure of the adsorbent itself also has an impact on the adsorption of the adsorbate. The adsorption of alkane molecules on brønsted acid sites is the key to the adsorption reaction. Therefore, it is essential to control the acidity of zeolite by regulating the Si/Al ratio. Although the adsorption selectivity is not sensitive to the Si/Al ratio, the distribution of Al plays a crucial role in the adsorption selectivity. Yang [39] reported that the change in Al distribution resulted in a two-fold increase in n-hexane adsorption selectivity. When the Si/Al ratio is large, the selectivity varied greatly with the distribution of aluminum. The positions of Al atoms at different T sites have a significant effect on the overall selectivity ratio. The Al atoms can synergistically enhance the adsorption of the central C–C bond when they are close together, resulting in a higher selectivity than isolated Al atoms. Controlling the location of Al in zeolites, such as MFI and other frameworks with heterogeneous pore systems, as well as a wide range of selectivity between different T-sites, would provide the opportunity to significantly improve the specific C-C bond to alkanes Adsorption selectivity. Robert F. D [40] reported the adsorption isotherms of silicalite-1 for α-alkanes and diols, and explained the adsorption mechanism in depth. It can be seen that the precise regulation of the atomic sites and texture composition in the catalyst greatly affects the adsorption performance of the adsorbent.

3.2. Aromatic Hydrocarbons

Aromatic hydrocarbons in petroleum mainly include polycyclic aromatic hydrocarbons (such as benzopyrene) and monocyclic aromatic hydrocarbons (benzene, toluene, xylene, etc.), while polycyclic aromatic hydrocarbons are organic compounds comprising two or more single ring molecules. Diesel produced by catalytic cracking is mostly inferior oil or heavy oil, therefore, recycling the aromatic hydrocarbons in diesel can not only improve the quality of diesel but also obtain the industrial raw material aromatics [41]. Commonly used methods for separating aromatic hydrocarbons include catalytic hydrogenation, adsorption separation, etc. At present, high-pressure hydrogenation is widely used in industry [42]. However, this method has problems such as high energy consumption, strict requirements, and poor product economy. The above problems can be effectively solved by the method of

adsorptive separation, which is mild, eco-friendly, and has high product quality. In addition, different adsorbents can be selected according to the different desired reactions, therefore, adsorptive separation is the most ideal separation mode. The currently applied adsorbents can be classified as follows:

3.2.1. Carbon Materials

Carbon materials include many classifications, such as common biochar, activated carbon (AC), and other configurations of carbon materials such as graphene, carbon nanotubes, and fullerenes [43–45]. Most carbon materials have porous structures, high specific surface areas, and can accommodate different adsorption molecules by introducing functional groups. Most carbon materials have a porous structure, high specific surface area, and can adapt to different adsorption molecules by introducing functional groups. These characteristics make carbon materials have good performance in the separation of aromatic hydrocarbons. Carbon materials commonly used for adsorptive separation include activated carbon, carbon nanotubes, and graphene materials, which mostly adsorb adsorbates via van der Waals forces, hydrogen bonding, or π-π interactions. Zhang [46] studied the adsorption behavior of five different carbon materials (particulate activated carbon material HD4,000, activated carbon ACF10, two single-walled carbon nanotubes SWNT, SWNT-HT, and multi-walled carbon nanotube MWNT) on aromatics. The factors affecting the adsorption behavior of carbon materials toward three aromatics (p-nitrotoluene PNT, p-xylene BP, and phenylphenol 2PP), the adsorption sites on different carbon materials, and the adsorption mechanism of adsorbates on the surface of carbon materials were quantitatively illustrated.

Figure 9 shows the adsorption isotherms of PNT, BP, and 2PP in different carbon materials. The authors fit the results using the FM adsorption model according to their modeling results, and the fit to the experimental data was better in the linear form (lnqe = lnkf + nlnce) than in the nonlinear form. The modified Freundlich model was adopted to normalize the C_E as well as the water-soluble S_W of adsorbate to obtain the equation:

$$q_e = K_{FS}(C_e/S_W)^n$$

q_e: the mass of solute adsorbed
C_e: the equilibrium concentration of the solute
S_w: water solubility
K_{FS} is a concentration-independent quantity that represents the effective adsorption capacity of the adsorbent, but it can only be used to estimate the effective adsorption amount when the C_e of the low-solubility adsorbent reaches saturation.

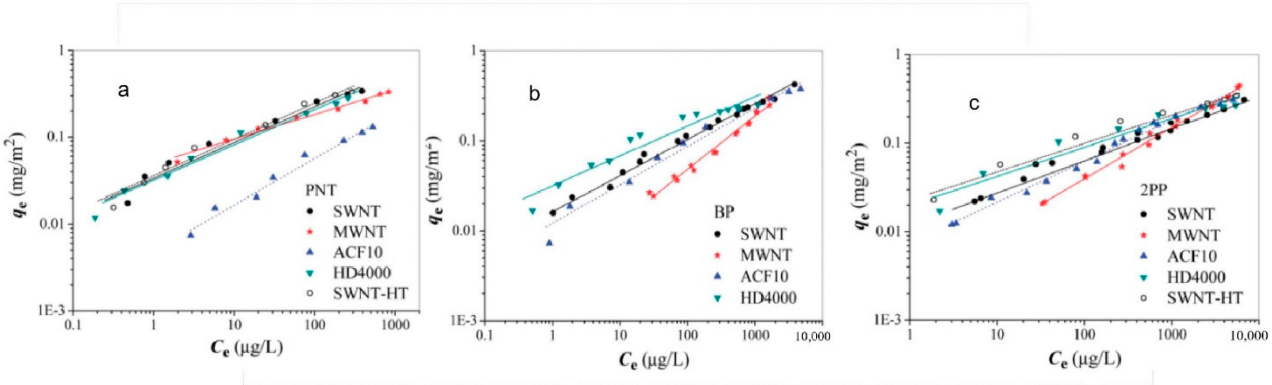


Figure 9. Adsorption isotherms of three organic aromatic compounds on different carbon materials [46]. Symbol: experimental data, line: linear fit of FM. ((**a**) p-nitrotoluene PNT, (**b**) p-xylene BP, (**c**) phenylphenol 2PP).

As can be seen in Figure 9, the adsorption isotherms of PNT on ACF10 (the pore is mostly microporous, mostly <1 nm) are significantly lower than that on other adsorbates (pore sizes larger than 1 nm diameter of PNT), and the adsorption isotherms of BP and 2PP are still in the fraction after the specific surface area normalization treatment, especially at low C_E. This indicates that the micropores and effective adsorption area play dominant roles in adsorption. In addition, the relationship between the adsorbed amount of activated carbon and the structural parameters of carbon was investigated, and V_{AOC}/V_{N2} was used to represent the effective coverage of organic aromatic compounds on the carbon surface, and V_{AOC}/V_t to represent the pore volume occupancy. It was concluded that at low molecular weight chemicals, the higher the microporous component of carbon, the higher the space volume component occupancy. This can be explained by the micropore effect: in the liquid-phase adsorption of low molecular weight chemicals, the adsorption potential overlap of the walls in the opposite position makes the micropores' adsorption energy much larger than the mesopores and macropores [47].

In addition to the micropore effect, there is also a sieving effect in the adsorption process of organic aromatic compounds—the width of the pores determines the entry of the adsorbate into the pores, and it changes with the shape of the adsorbent [48]. Specifically, for cylindrical or ellipsoid adsorbents, the second width of the adsorbate, such as the size of the PNT molecule (11.7 Å × *8.0 Å × 3.4 Å), determines whether it can enter the adsorbent, such as CNTs and ACF10, while for interstitial adsorbates, the factor that determines adsorbate entry is the smallest size, such as HD4,000. In ACF10, since 70% of the pores are smaller than 1 nm, and the second size of PNT is 0.8 nm, the sieving effect is more obvious in the adsorption effect of ACF10, which is also consistent with the fitting results of the Freundlich model above.

Mazen Khaled [49] also studied the separation behavior of different carbon materials (activated carbon AC, carbon nanotube MWCNT, and graphene oxide GO) for thiophene and dibenzothiophene DBT mixed into n-hexane, and studied the effect of stirring speed, adsorbent mass loading, contact time and adsorption kinetics and initial organosulfide concentration on adsorption. The results show that the adsorption capacity of graphene oxide and carbon nanotubes is weaker than that of activated carbon adsorption desulfurization, but compared with activated carbon, their adsorption speed is faster and the volume quality is lower, which make it can be used for adsorption desulfurization of automobiles and fuel cells, so there is more practical economic value. The author also uses the Freundlich model to fit the adsorption kinetics to judge the applicability of the adsorbent to the adsorbate. For DBT, the obtained isomerism value (1/n) exceeds 1, indicating that carbon nanotubes and the adsorption effect of graphene oxide on it are strong, which are 23.42 and 22.73 mg/g, respectively. The isomerism value (1/n) of thiophene is less than 1, indicating that these adsorbents are not suitable for the adsorption of thiophene.

Activated carbon (AC) is the most widely reported carbon adsorption material, which has been widely commercialized due to its multiple sources and high economic value. Chen et al. [50] reported the synthesis of magnetically activated carbon nanocomposites (MNPsGTAC) from green tea waste, with a specific surface of 118.8 $m^2\ g^{-1}$ and a particle size of 8.6 nm, which were used to evaluate the adsorption efficiency of four priority polycyclic aromatic hydrocarbons (PAHs), and the catalyst could be completely recovered through acetonitrile. For mineral springs, the removal rates of polycyclic aromatic hydrocarbons are 86–98% and 72–89%, respectively. For tap water and river water, the polycyclic aromatic hydrocarbons are completely removed, showing high adsorption efficiency. However, from the above discussion, the adsorption efficiency of graphene and carbon nanotubes is higher than that of AC, which is mainly due to higher specific surface area, stronger hydrogen bonds, and π-π interaction with pollutants. For example, naphthalene molecules contain C-C or two benzene rings containing π electrons. Each carbon atom in the carbon nanotube structure has a π electron orbital perpendicular to the surface of the carbon nanotube, so it can form π-π bonds with CNTs. In addition, there are other adsorption sites, such as the defects of adsorbed polycyclic aromatic hydrocarbons, and the gaps and grooves between

CNTs bundles, which can be effective sites for adsorbing aromatic hydrocarbons [51]. Zhang et al. [52] reported on the efficient adsorption of phenanthrene in water by magnetic carbon nanotubes (MCNMs) and proved that the adsorption process of phenanthrene on these MCNMs is a spontaneous, exothermic, and entropy reduction process, which can still be recovered and reused after the treatment of n-hexane. Bayazit et al. [53] used graphene plate metal-organic network nanocomposite to remove naphthalene. The experimental results showed that 0.075 mg GNP/MIL-101 had the highest adsorption efficiency for naphthalene, up to 93% at 298 K.

3.2.2. Silicon-Based Materials

As the second most abundant element on the earth, silicon has been widely concerned because of its wide source, friendly environment, and high economic benefits [54]. Many materials with adsorption properties can be obtained by silicon precursor, such as molecular sieve, ordered mesoporous silica, gel, etc. [55–57], which usually have high specific surface area, high pore size ratio, and low density, so they can be used as good adsorbents. Cesar M.C. Filho [58] synthesized MTMS aerogel gel materials to separate hydrocarbon materials from petroleum, including mixed solutions of monocyclic aromatic hydrocarbons MAHs (benzene, toluene, and xylene) and polycyclic aromatic hydrocarbons PAHs (pyrene, benzofluoranthene, and benzopyrene) to obtain adsorption isotherms, They also studied the interaction between aerogels and aromatic compounds during adsorption and desorption and sought the adsorbent materials most suitable for different adsorbents.

Figure 10 showed the fitting data of different aromatic compounds using different models. The adsorbate adsorption curve presented a concave profile, and with the continuous increase of adsorbate equilibrium CE, the QE value also increased sharply, which was different from the previous convex profile of benzene and toluene [59]. Therefore, the authors discussed the adsorption parameters of the two adsorption models. Notably, the fitting effect of the graph that the simulation effect of BET is better, while the isomerism value obtained by fitting the Freundlich model (1/n) is greater than 1, which indicates that there are two possibilities for the adsorption mechanism of aerogels for aromatic compounds, one is a multilayer adsorption mechanism, and the other may be dissolved in a solvent into the aerogel and adsorbed from BET. From the bet adsorption model, there is a single-layer adsorption in the early stage (for polycyclic aromatic hydrocarbons, C_E is < 12 mg L^{-1}, while for monocyclic aromatic hydrocarbons, CE is < 2 mg L^{-1}), and then the QE value increases sharply with the increase of CE value, which also indicates that there is multi-layer physical adsorption [60].

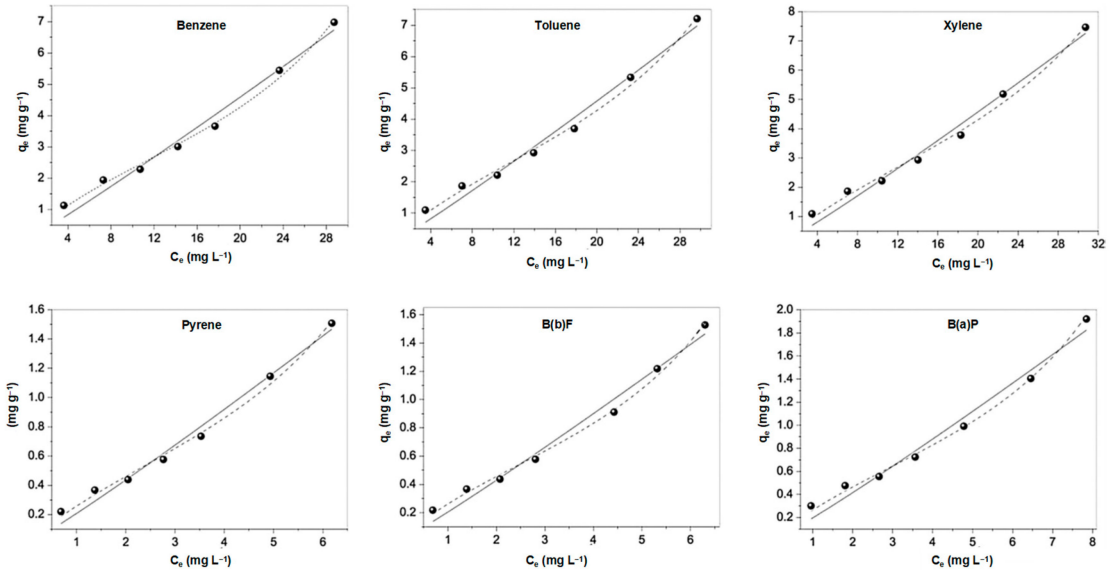


Figure 10. Adsorption isotherms of different aromatic hydrocarbon compounds at 25 °C [58] (The solid line is the fit of the Freundlich model, and the dashed line is the fit of the BET model).

Figure 11 showed the adsorption capacity relationship obtained according to the mixed aromatics solutions with different initial concentrations. With the increase of the initial concentration of aromatic compounds, the adsorption capacity of the aromatic compounds also increases. However, it should be noted that no matter how the initial content changes, the percentage of hydrocarbon adsorption of each component remains unchanged and is basically arranged in the order of Xyl > Tol > Ben >> B(a)P > B(b)F ≈ Pyr. The adsorption percentage of monocyclic aromatic hydrocarbons is much higher than that of polycyclic aromatic hydrocarbons, which may be due to the difference in the adsorption of the two types of aromatic hydrocarbons on the aerogel gel surface. The biggest difference between the two aromatic hydrocarbons lies in their hydrophobicity, and the increase in adsorption capacity has the same correlation with hydrophobicity. This is mainly because the surface of aerogel gel is hydrophobic, and the hydrophobicity of monocyclic aromatic hydrocarbons is greater than that of polycyclic aromatic hydrocarbons, so the adsorption percentage of monocyclic aromatic hydrocarbons is also higher than that of polycyclic aromatic hydrocarbons.

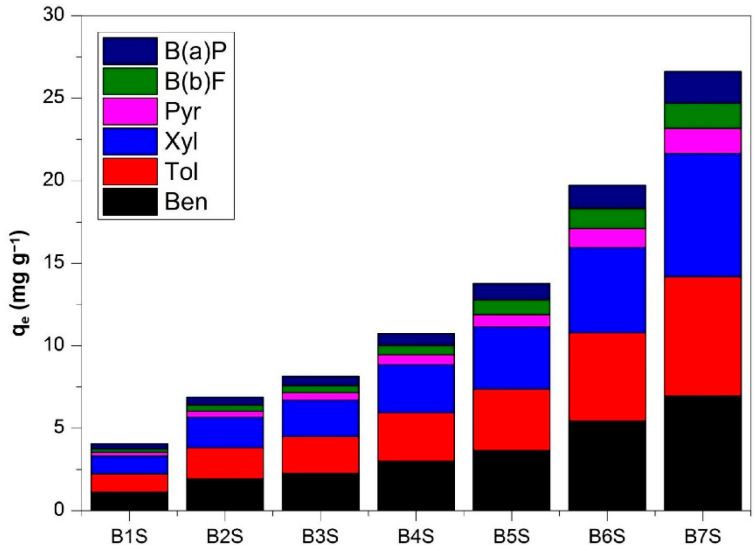


Figure 11. Dependence of adsorption capacity of MTMS-aerogel on the initial concentration of different mixtures [58].

The desorption process is a process that can reevaluate the performance of the adsorbent. The mechanism of adsorption can be better understood by studying the desorption process. Figure 12 showed the desorption results of different aromatics by aerogel. With the increase of initial concentration, polycyclic aromatic hydrocarbons are first desorbed, while monocyclic aromatic hydrocarbons (benzene, toluene, xylene) are largely retained in the aerogel gel, which is consistent with the BET results, that is, in the process of adsorption, small aromatic molecules on the surface of aerogel gel firstly and following the multi-layer adsorption mechanism of polycyclic aromatic hydrocarbons. In the process of desorption, the π-π stacking effect of inner monocyclic aromatic hydrocarbons is stronger than that of outer polycyclic aromatic hydrocarbons, so it is more difficult to desorption monocyclic aromatic hydrocarbons macroscopically, to achieve the effect of separation.

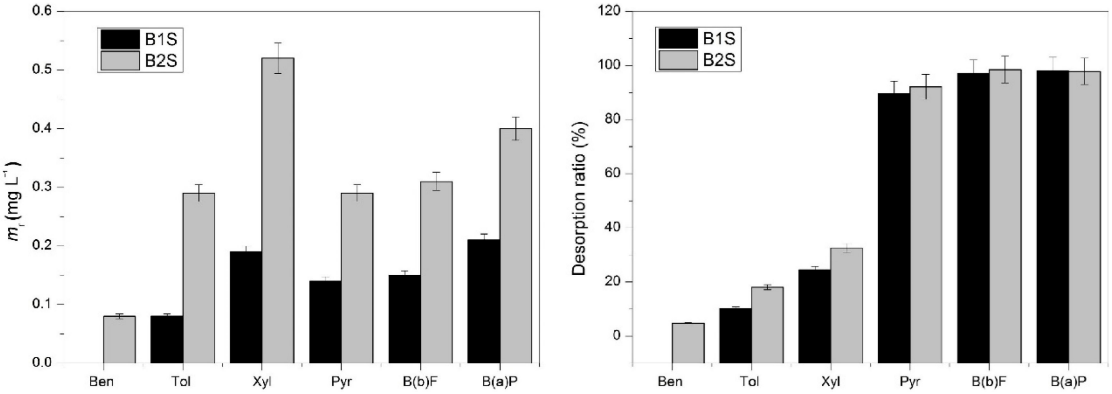


Figure 12. Desorption results of different aromatics by MTMS-aerogel [58] (Methanol:water = 70:30, room temperature, 307 h contact).

Ordered mesoporous silica has also been widely used as an adsorbent for arenes and phenols due to its uniform pore structure, tunable pore size, high specific surface area, and high mass transfer efficiency. Moreover, its performance for specific hydrocarbons can be optimized by metal modification. For example, SBA-15 with framework Fe (III) can be applied to the removal of pyrene and Cu (II) in water [61]. Protonated Fe (III) acts as an adsorption site, while the bridge bond between pyrene and Cu (II) further promotes adsorption. Shajesh P. [62] reported the adsorption of various organic pollutants (chloroform, ethylene glycol, acetonitrile, ethyl acetate, xylene, acetone, toluene, dimethyl sulfoxide, 2-butoxyethanol) with mesoporous silica colloids (pore size ~3 nm, specific surface area >1100 m^2/g). The adsorption efficiency displays a negative correlation with the polarity of organic components, which is similar to classical adsorbents. Furthermore, enhancing the hydrophobicity of the adsorbent with organsilanes promotes the adsorption capacity and the regeneration of diffusion-assisted adsorbent molecules.

In addition, the molecular sieve can also be used for the adsorption and desorption of hydrocarbon molecules in petroleum. Yang [63] used Cu^+Y molecular sieves to adsorb hydrocarbons by π complexation with N-containing compounds. During the experiment. They also found its good adsorption potential for S-containing compounds. However, its low maximum adsorption capacity (3 mg/g of nitrogen-containing compounds) means that finding materials with high adsorption performance is still a serious challenge.

3.2.3. Polymer Adsorption Technology

Polymer adsorption technology has been widely used for the adsorptive separation of gaseous hydrocarbons for decades benefiting from the proper interaction between polymer and adsorbate [64,65]. A high specific surface area is necessary for this type of material due to its dependence on capillarity. The adsorption occurs not only on the polymer surface, but also inside the polymer. Therefore, it is necessary to prevent polymer swelling by making the polymer into a three-dimensional network cross-linked structure [66]. Changwoo Nam [67] discussed the performance of "Petrogel" polyethylene-based hydrophobic adsorbent on adsorbing aromatic hydrocarbons in water. They found that materials with high density, high melting temperature, and high crystallinity tended to have lower adsorption capacity. Meanwhile, oil products with lower molecular weight such as toluene and diesel show high adsorption capacity compared to ANS crude oil with larger molecular weight. A-6-P with a more branched chain, low density, low melting temperature, and low crystallinity could adsorb more than 17 times its weight in toluene, 7.6 times in diesel oil, and 2.5 times in ANS crude oil. Non-crystalline x-D-DVB also shows higher toluene adsorption capacity compared to crystalline LLDPE. On this basis, Changwoo Nam [68] obtained "i-Petrogel" by mixing a semi-crystalline linear low-density polyethylene (LLDPE) thermoplastic and a thermally cross-linked polyethylene (1-decane) ene-co-divinylbenzene). This absorbent

shows high adsorption capacity (40 times its weight), high selectivity, and high adsorption rate for crude oil from low-temperature frozen soil.

3.2.4. Metal-Organic Frameworks (MOFs)

Attributing to ultra-high specific surface area (up to 9000 m^2/g), high porosity [69], and controlled functional groups, metal-organic frameworks (MOFs) have been widely applied to hydrocarbon adsorption [70]. Michael Maes [71] used mesoporous carboxylate with a different topological structure to adsorb benzothiophene and dibenzothiophene. They found that octahedral trimer MOFs with Lewis acid sites had high selectivity for N-containing aromatics. These MOFs showed high performance and good reproducibility even under the detrimental influence of solvent coadsorption.

Porous $Zn_4O(BDC)_3$, also known as MOF-5, which is a typical isoreticular metal-organic framework (IRMOF), is also widely used in the adsorption of aromatic hydrocarbons. W. Makowski [72] studied the adsorption behavior of different hydrocarbon molecules, such as n-alkane, isooctane, benzene, toluene, and xylene. They found an unusual thermal desorption profile, which was different from the five standard isotherm when the adsorbed molecules were large. Further investigation should be made to explain its particular adsorption characteristics.

3.2.5. Chitosan

As a natural polysaccharide, chitosan is a cheap adsorption material extracted from seafood shells and natural substances. Owing to its substantial hydroxyl functional groups, it is widely applied to PAHs adsorption [73]. Specific demands for different adsorbents can be satisfied by blending or crosslinking chitosan with other polymers. S. Bibi [74] synthesized a membrane composed of chitosan, polyvinylpyrrolidone (PVP), and carbon nanotubes (CNTs) with a specific surface of 253 m^2/g. Moreover, carbon nanotubes with different functional groups were obtained by gamma-ray irradiation for NAPH adsorption. The effective removal rates were 93% and 97% at 120 min and 150 min, respectively. The rapid adsorption of aromatic hydrocarbons can be attributed to the strong π-π interaction between aromatic hydrocarbons (naphthalene used in this paper) and the surface of hydrophobic carbon materials.

4. Summary

In this review, the rules and mechanisms of adsorption and desorption of hydrocarbon molecules are comprehensively described. It can be seen that many materials can be used in the adsorption of hydrocarbon molecules. The adsorbents can be selected according to the characteristic of the adsorbate. With further research, the emergence of composite adsorbents has greatly promoted the adsorption efficiency of hydrocarbon molecules. Composite materials are known to possess physical and chemical properties superior to their precursor and conventional porous materials. They have the advantages of ultra-high porosity and specific surface area, high crystallinity, uniform surface morphology, and high chemical and thermal stability. However, it is undeniable that there are still many challenges: (1) regulation of grain size and morphology of crystalline adsorbents, (2) control of pore size distribution and surface properties of amorphous adsorbent materials, (3) precise regulation of pore size of shape-selective adsorbent materials, (4) balance the interaction with adsorbent and adsorbate.

Huge economic profits can be brought for the enterprise by developing green and efficient adsorption separation of special materials and molecular-level adsorption materials, managing the oil products at a molecular level, and realizing targeted treatment and high-quality utilization. At the same time, the separation technology with molecular-level adsorption materials at the core will build a molecular-level management technology platform, promote the development of separation and refining technology, reduce energy consumption and carbon dioxide emission and avoid pollution.

Author Contributions: H.Y.: Conceptualization, Supervision, Investigation, J.Z.: Investigation. C.G.: Investigation. B.L. (Bin Li): Conceptualization, Writing—original draft. B.L. (Ben Li): Investigation. X.Z.: Investigation, Writing—original draft. T.C.: Investigation All authors have read and agreed to the published version of the manuscript.

Funding: This work is supported by grant CNOOC-ZDXM2-0002-2020-TJY of CNOOC.

Conflicts of Interest: The authors declare no conflict of interest.

References

1. Dai, H.J.; Li, H.L.; Zhou, G.W.; He, Y.F.; Zhou, W.M.; Chen, W.; Shi, H. X Degradation characteristics of organic pollutants in the treatment of printing and dyeing wastewater by GC-MS. *J. Zhejiang Univ. (Sci. Ed.)* **2014**, *41*, 72–77.
2. Long, R.Q.; Yang, R.T. Carbon nanotubes as superior sorbent for dioxin removal. *J. Am. Chem. Soc.* **2001**, *123*, 2058–2059. [CrossRef] [PubMed]
3. Fan, R.J.; Cui, X.Y. Bioavailability of persistent organic pollutants in soil. *Environ. Ecol.* **2021**, *3*, 15–26.
4. Huang, W.Q.; Tian, Q.; Zhao, S.H.; Gao, X.Q.; Lu, X.W.; Wang, Y.Y. Evaporative oil and gas adsorption separation and recovery technology. *Oil Gas Storage Transp.* **1998**, *12*, 47–50.
5. Huang, W.Q.; Zhong, Q. Analysis and comparison of oil and gas recovery technology. *Chem. Eng.* **2005**, *5*, 56–59+68.
6. Ding, L.S. *Basic Research on the Removal of Aromatics from Simulated Catalytically Cracked Diesel Fuel*; China University of Petroleum: Beijing, China, 2018.
7. Li, H.; Eddaoudi, M.; O'Keeffe, M.; Yaghi, O.M. Design and synthesis of an exceptionally stable and highly porous metal-organic framework. *Nature* **1999**, *402*, 276–279. [CrossRef]
8. Ni, Q.; Lai, J.B.; Peng, D.Y.; Guan, C.S.; Long, J. Research progress of ionic liquid extraction and separation of hydrocarbon compounds. *Prog. Chem. Ind.* **2021**, *6*, 1–11.
9. Yin, M.F.; Tang, Z.; Zhang, R.; Liu, Z.C.; Liu, H.Y.; Xu, C.M.; Meng, X. H Separation of n-octane/o-xylene by ionic liquid liquid-liquid extraction. *Chin. J. Chem. Eng.* **2021**, *72*, 1–9.
10. Jiang, X.; Yang, F.C.; Guo, Z.G. Superwetting surfaces for filtration separation of high-viscosity raw petroleum/water mixtures. *J. Mater. Chem. A* **2022**, *10*, 14273–14292. [CrossRef]
11. Saien, J.; Kharazi, M.; Yarie, M.; Zolfigol, M.A. A Systematic investigation of a surfactant type nano gemini ionic liquid and simultaneous abnormal salts effects on the crude oil/water interfacial tension. *Ind. Eng. Chem. Res.* **2019**, *58*, 3583–3594. [CrossRef]
12. Nazhipkyzy, M.; Assylkhanova, D.; Araylim, N.; Seitkazinova, A.; Özsin, G.; Varol, E.A. Effective separation of petroleum oil-water mixtures via flexible and re-usable hydrophobic soot-coated melamine sponge. *J. Water Process. Eng.* **2022**, *49*, 103032. [CrossRef]
13. Chuah, C.Y.; Bae, T.-H. Recent advances in mixed-matrix membranes for light hydrocarbon (c(1)–c(3)) separation. *Membranes* **2022**, *12*, 201. [CrossRef] [PubMed]
14. Zhang, Y.; Tao, S. Global atmospheric emission inventory of polycyclic aromatic hydrocarbons (PAHs) for 2004. *Atmos. Environ.* **2009**, *43*, 812–819. [CrossRef]
15. Cao, J.F.; Liu, W.; Liao, J.F.; Xie, W.J.; Huang, W. Prediction of Product Properties of Catalytic Diesel Hydrocracking with Different Aromatic Mass Fractions. *Contemp. Chem. Ind.* **2021**, *50*, 1897–1899+1904.
16. Sun, H.; Shen, B.X. Effect of Binder on Adsorption of N-alkanes on 5A Molecular Sieve. *Petrochem. Ind.* **2011**, *40*, 279–284.
17. Broughton, D.B.; Gerhold, C.G. Continuous Sorption Process Employing Fixed Bed of Sorbent and Moving Inlets and Outlets. U.S. Patent 2,985,589, 23 May 1961.
18. Huo, Q.; Dou, T.; Zhao, Z.; Pan, H. Synthesis and application of a novel mesoporous zeolite L in the catalyst for the HDS of FCC gasoline. *Appl. Catal. A Gen.* **2010**, *381*, 101–108. [CrossRef]
19. Ban, S.; Van Laak, A.; De Jongh, P.E.; Van der Eerden, J.P.; Vlugt, T.J. Adsorption selectivity of benzene/propene mixtures for various zeolites. *J. Phys. Chem. C* **2007**, *111*, 17241–17248. [CrossRef]
20. Costa, A.A.; Wilson, W.B.; Wang, H.; Campiglia, A.D.; Dias, J.A.; Dias, S.C. Comparison of BEA, USY and ZSM-5 for the quantitative extraction of polycyclic aromatic hydrocarbons from water samples. *Microporous Mesoporous Mater.* **2012**, *149*, 186–192. [CrossRef]
21. Gao, F.; Wang, Y.; Wang, S. Selective adsorption of CO on CuCl/Y adsorbent prepared using $CuCl_2$ as precursor: Equilibrium and thermodynamics. *Chem. Eng. J.* **2016**, *290*, 418–427. [CrossRef]
22. Song, R.T.; Yao, J.; Yang, M.; Ye, Z.B. Insights into High-Performance and Selective Elimination of Cationic Dye from Multicomponent Systems by Using Fe-Based Metal–Organic Frameworks. *Langmuir* **2022**, *38*, 9400–9409. [CrossRef]
23. Gu, J.J.; Gao, Y.M.; Zhang, J.L.; Li, W.; Dong, Y.Z.; Han, Y. Hydrochlorination of Acetylene Catalyzed by an Activated Carbon-Supported Ammonium Hexachlororuthenate Complex. *Catalysts* **2017**, *7*, 17. [CrossRef]
24. Jiang, Y.; He, Y.H.; Gao, H.Y. Recent progress in porous intermetallics: Synthesis mechanism, pore structure, and material properties. *J. Mater. Sci. Technol.* **2021**, *74*, 89–104. [CrossRef]
25. Qu, D.; Feng, X.; Li, N.; Ma, X.; Shang, C.; Chen, X.D. Adsorption of heterocyclic sulfur and nitrogen compounds in liquid hydrocarbons on activated carbons modified by oxidation: Capacity, selectivity and mechanism. *RSC Adv.* **2016**, *6*, 41982–41990. [CrossRef]

26. Pang, Y.; Huang, Y.; Li, W.; Feng, L.; Shen, X. Conjugated polyelectrolyte/graphene multilayer films for simultaneous electrochemical sensing of three monohydroxylated polycyclic aromatic hydrocarbons. *ACS Appl. Nano Mater.* **2019**, *2*, 7785–7794. [CrossRef]
27. Tan, Y.; Chen, L.; Wu, F.; Huang, B.; Liao, Z.; Yu, Z.; Hu, L.; Zhou, Y.; Chen, Y. Regulation of the polar groups in n-Type conjugated polyelectrolytes as electron transfer layer for inverted polymer solar cells. *Macromolecules* **2018**, *51*, 8197–8204. [CrossRef]
28. Costa, A.S.; Romão, L.P.; Araújo, B.R.; Lucas, S.C.; Maciel, S.T.; Wisniewski, A., Jr.; Alexandre, M.D. Environmental strategies to remove volatile aromatic fractions (BTEX) from petroleum industry wastewater using biomass. *Bioresour. Technol.* **2012**, *105*, 31–39. [CrossRef]
29. Varjani, S.J.; Upasani, V.N. Core flood study for enhanced oil recovery through ex-situ bioaugmentation with thermo- and halo-tolerant rhamnolipid produced by Pseudomonas aeruginosa NCIM 5514. *Bioresour. Technol.* **2016**, *220*, 175–182. [CrossRef]
30. Liu, S.; Chen, Y.; Yue, B.; Nie, Y.; Chai, Y.; Wu, G.; Li, J.; Han, X.; Day, S.J.; Thompson, S.P.; et al. Cascade adsorptive separation of light hydrocarbons by commercial zeolites. *J. Energy Chem.* **2022**, *72*, 299–305. [CrossRef]
31. Yao, Z.L.; Zhao, Y.Z. Advances in Adsorption and Separation Technology of N-alkanes. *Prog. Chem. Ind.* **2003**, *22*, 589–592.
32. Cao, D.; Li, Z.; Wang, Z.; Wang, H.; Gao, S.; Wang, Y.; Shi, Y.; Qiu, J.; Zhao, Y.; Wang, J. Highly Dispersed Ionic Liquids in Mesoporous Molecular Sieves Enable a Record NH_3 Absorption. *ACS Sustain. Chem. Eng.* **2021**, *9*, 16363–16372. [CrossRef]
33. Gao, S.; Liu, Z.; Xu, S.; Zheng, A.; Wu, P.; Li, B.; Yuan, X.; Wei, Y.; Liu, Z. Cavity-controlled diffusion in 8-membered ring molecular sieve catalysts for shape selective strategy. *J. Catal.* **2019**, *37*, 51–62. [CrossRef]
34. Kang, D.W.; Ju, S.E.; Kim, D.W.; Kang, M.; Kim, H.; Hong, C.S. Emerging porous materials and their composites for NH_3 gas removal. *Adv. Sci.* **2020**, *7*, 2002142. [CrossRef] [PubMed]
35. Cao, J.; Shen, B.X. Optimized utilization of naphtha: Liquid adsorption separation of linear paraffins in naphtha with n-pentane as the desorbent. *Energy Sources Part A Recovery Util. Environ. Eff.* **2013**, *35*, 235–245. [CrossRef]
36. Liu, Y.S.; Wang, H.C.; Qiao, X.F.; Yang, Y.Q.; Wang, D.H.; Wang, H.G. Study on adsorption and separation of n-alkanes with 5A molecular sieve adsorbent. *Petrochemical* **2021**, *50*, 534.
37. Santi, K. *Zeolites in Industrial Separation and Catalysis*; John Wiley & Sons: Hoboken, NJ, USA, 2010; p. 219.
38. He, J.; Yan, A.Z. Properties of 5A Dewaxed Molecular Sieve IV. Effect of Ca^{2+} Exchange Degree on Desorption and Diffusion in n-alkane Molecular Sieve. *Chin. J. Pet.* **1995**, *11*, 13–20.
39. Yang, C.T.; Janda, A.; Bell, A.T.; Lin, L.C. Atomistic investigations of the effects of Si/Al ratio and Al distribution on the adsorption selectivity of n-Alkanes in Brønsted Acid zeolites. *J. Phys. Chem. C* **2018**, *122*, 9397–9410. [CrossRef]
40. Robert, F.D.; Bahman, E.; Matheus, D.M. Understanding the unique sorption of alkane-α, ω-diols in silicalite-1. *J. Chem. Phys.* **2018**, *149*, 072331.
41. Wang, L.Y.; Yang, G.M.; Xin, J. Research progress on the removal of aromatic hydrocarbons from diesel fuel by adsorption process. *Petrochem. Technol. Appl.* **2021**, *39*, 66–69.
42. Xu, Y.Q.; Wang, Z.Y.; Pang, X.Y.; Xiao, L.G. Analysis on the scheme of diesel hydrocracking to reduce diesel-gasoline ratio. *Zhongwai Energy* **2016**, *21*, 85–89.
43. Zhang, C.; Wang, B.; Xiang, J.; Su, C.; Mu, C.; Wen, F.; Liu, Z. Microwave absorption properties of CoS_2 nanocrystals embedded into reduced graphene oxide. *ACS Appl. Mater. Interfaces* **2017**, *9*, 28868–28875. [CrossRef]
44. Al-Jammal, N.; Abdullah, T.A.; Juzsakova, T.; Zsirka, B.; Cretescu, I.; Vágvölgyi, V.; Sebestyén, V.; Le Phuoc, C.; Rasheed, R.T.; Domokos, E. Functionalized carbon nanotubes for hydrocarbon removal from water. *J. Environ. Chem. Eng.* **2020**, *8*, 103570. [CrossRef]
45. Wu, B.; Jiang, L.; Luo, Y.; Wang, C.R. The Effect of the Polyaromatic Hydrocarbon in the Formation of Fullerenes. *Angew. Chem. Int. Ed.* **2020**, *59*, 3942–3947. [CrossRef]
46. Zhang, S.; Shao, T.; Kose, H.S.; Karanfil, T. Adsorption of aromatic compounds by carbonaceous adsorbents: A comparative study on granular activated carbon, activated carbon fiber, and carbon nanotubes. *Environ. Sci. Technol.* **2010**, *44*, 6377–6383. [CrossRef]
47. Daley, M.A.; Tandon, D.; Economy, J.; Hippo, E.J. Elucidating the porous structure of activated carbon fibers using direct and indirect methods. *Carbon* **1996**, *34*, 1191–1200. [CrossRef]
48. Bandosz, T.J. *Activated Carbon Surfaces in Environmental Remediation*; Elsevier: Amsterdam, The Netherlands, 2006.
49. Khaled, M. Adsorption performance of multiwall carbon nanotubes and graphene oxide for removal of thiophene and dibenzothiophene from model diesel fuel. *Res. Chem. Intermed.* **2015**, *41*, 9817–9833. [CrossRef]
50. Inbaraj, B.S.; Sridhar, K.; Chen, B.H. Removal of polycyclic aromatic hydrocarbons from water by magnetic activated carbon nanocomposite from green tea waste. *J. Hazard Mater.* **2021**, *415*, 125701. [CrossRef]
51. Pan, B.; Xing, B.X. Adsorption mechanisms of organic chemicals on carbon nanotubes. *Environ. Sci. Technol.* **2008**, *42*, 9005–9013. [CrossRef]
52. Zhang, J.; Li, R.; Ding, G.; Wang, Y.; Wang, C. Sorptive removal of phenanthrene from water by magnetic carbon nanomaterials. *J. Mol. Liq.* **2019**, *293*, 111540. [CrossRef]
53. Bayazit, Ş.S.; Yildiz, M.; Aşçi, Y.S.; Şahin, M.; Bener, M.; Eğlence, S.; Salam, M.A. Rapid adsorptive removal of naphthalene from water using graphene nanoplatelet/MIL-101 (Cr) nanocomposite. *J. Alloys Compd.* **2017**, *701*, 740–749. [CrossRef]
54. Aksu, Z.; Yener, J. A comparative adsorption/biosorption study of mono-chlorinated phenols onto various sorbents. *Waste Manag.* **2001**, *21*, 695–702. [CrossRef]
55. Elangovan, S.P.; Ogura, M.; Zhang, Y.; Chino, N.; Okubo, T. Silicoaluminophosphate molecular sieves as a hydrocarbon trap. *Appl. Catal. B* **2005**, *57*, 31–36. [CrossRef]

56. Maretto, M.; Vignola, R.; Williams, C.D.; Bagatin, R.; Latini, A.; Papini, M.P. Adsorption of hydrocarbons from industrial wastewater onto a silica mesoporous material: Structural and thermal study. *Micropor. Mesopor. Mater.* **2015**, *203*, 139–150. [CrossRef]
57. Zhan, C.; Jana, S.C. Shrinkage reduced polyimide-graphene oxide composite aerogel for oil absorption. *Microporous Mesoporous Mater.* **2020**, *307*, 110501. [CrossRef]
58. Cesar Filho, M.C.; Matias, T.; Duraes, L.; Valente, A.J. Efficient simultaneous removal of petroleum hydrocarbon pollutants by a hydrophobic silica aerogel-like material. *Colloids Surf. A Physicochem. Eng. Asp.* **2017**, *520*, 550–560. [CrossRef]
59. Štandeker, S.; Novak, Z.; Knez, Ž. Removal of BTEX vapours from waste gas streams using silica aerogels of different hydrophobicity. *J. Hazard. Mater.* **2009**, *165*, 1114–1118. [CrossRef]
60. Zhang, L.; Zeng, Y.; Cheng, Z. Removal of heavy metal ions using chitosan and modified chitosan: A review. *J. Mol. Liq.* **2016**, *214*, 175–191. [CrossRef]
61. Zhang, Z.; Hou, X.; Zhang, X.; Li, H. The synergistic adsorption of pyrene and copper onto Fe (III) functionalized mesoporous silica from aqueous solution. *Colloids Surf. A Physicochem. Eng. Asp.* **2017**, *520*, 39–45. [CrossRef]
62. Palantavida, S.; Peng, B.; Sokolov, I. Absorption of organic compounds by mesoporous silica discoids. *Micropor Mesopor Mat.* **2020**, *306*, 110379. [CrossRef]
63. Hernández Maldonado, A.J.; Yang, R.T. Denitrogenation of transportation fuels by zeolites at ambient temperature and pressure. *Angew. Chem.* **2004**, *116*, 1022–1024. [CrossRef]
64. Ono, T.; Sugimoto, T.; Shinkai, S.; Sada, K. Lipophilic polyelectrolyte Gels as super-absorbent polymers for nonpolar organic solvents. *Nat. Mater.* **2007**, *6*, 429–433. [CrossRef]
65. Chung, T.C.M.; Jeong, Y.; Chen, Q.; Kleinhammes, A.; Wu, Y. Synthesis of microporous boron-substituted Carbon (B/C) materials using polymeric precursors for hydrogen physisorption. *J. Am. Chem. Soc.* **2008**, *130*, 6668–6669. [CrossRef]
66. Xue, W.; Hamley, I.W.; Huglin, M.B. Rapid swelling and deswelling of thermoreversible hydrophobically modified poly(N-Isopropylacrylamide) hydrogels prepared by freezing polymerisation. *Polymer* **2002**, *43*, 5181–5186. [CrossRef]
67. Nam, C.; Li, H.X.; Chung, T.C.M. Petrogel: New hydrocarbon (petroleum) absrbent based on polyolefin polymers. *Macromolecules* **2016**, *49*, 5427–5437. [CrossRef]
68. Nam, C.; Li, H.X.; Chung, T.C.M. Practical petroleum spill recovery by a combination of polyolefin absorbent and mechanical skimmer. *ACS Sustain. Chem. Eng.* **2018**, *6*, 12036–12045. [CrossRef]
69. Jiang, D.; Chen, M.; Wang, H.; Zeng, G.; Huang, D.; Cheng, M.; Liu, Y.; Xue, W.; Wang, Z. The application of different typological and structural MOFs-based materials for the dyes adsorption. *Coord. Chem. Rev.* **2019**, *380*, 471–483. [CrossRef]
70. Zou, D.; Liu, D. Understanding the modifications and applications of highly stable porous frameworks via UiO-66. *Mater. Today Chem.* **2019**, *12*, 139–165. [CrossRef]
71. Maes, M.; Trekels, M.; Boulhout, M.; Schouteden, S.; Vermoortele, F.; Alaerts, L.; Heurtaux, D.; Seo, Y.K.; Hwang, Y.K.; Chang, J.S.; et al. Selective removal of N-heterocyclic aromatic contaminants from fuels by Lewis acidic metal–organic frameworks. *Angew. Chem. Int. Ed.* **2011**, *50*, 4210–4214. [CrossRef]
72. Makowski, W.; Mańko, M.; Zabierowski, P.; Mlekodaj, K.; Majda, D.; Szklarzewicz, J.; Łasocha, W. Unusual adsorption behavior of volatile hydrocarbons on MOF-5 studied using thermodesorption methods. *Thermochim. Acta* **2014**, *587*, 1–10. [CrossRef]
73. Zango, Z.U.; Sambudi, N.S.; Jumbri, K.; Ramli, A.; Abu Bakar, N.H.; Saad, B.; Rozaini, M.N.; Isiyaka, H.A.; Osman, A.M.; Sulieman, A. An overview and evaluation of highly porous adsorbent materials for polycyclic aromatic hydrocarbons and phenols removal from wastewater. *Water* **2020**, *12*, 2921. [CrossRef]
74. Bibi, S.; Yasin, T.; Hassan, S.; Riaz, M.; Nawaz, M. Chitosan/CNTs green nanocomposite membrane: Synthesis, swelling and polyaromatic hydrocarbons removal. *Mater. Sci. Eng. C* **2015**, *46*, 359–365. [CrossRef]

Disclaimer/Publisher's Note: The statements, opinions and data contained in all publications are solely those of the individual author(s) and contributor(s) and not of MDPI and/or the editor(s). MDPI and/or the editor(s) disclaim responsibility for any injury to people or property resulting from any ideas, methods, instructions or products referred to in the content.